Familial atrial fibrillation mutation M1875T-SCN5A increases early sodium current and dampens the effect of flecainide

Molly O'Reilly [1,2†], Laura C. Sommerfeld [1,3,4†], C. O'Shea [1], S. Broadway-Stringer [1], S. Andaleeb [1], J.S. Reyat [1], S.N. Kabir [1], D. Stastny [3], A. Malinova [1], D. Delbue [3,4], L. Fortmueller [3,4], K. Gehmlich [1,6], D. Pavlovic [1], B.V. Skryabin [7], A.P. Holmes [1,8], P. Kirchhof [1,4,5], and L. Fabritz [1,3,4,5]*

[1]Institute of Cardiovascular Sciences, University of Birmingham, Edgbaston, Wolfson Drive, Birmingham B15 2TT, UK; [2]Department of Experimental Cardiology, Academic Medical Center, Amsterdam, The Netherlands; [3]University Center of Cardiovascular Science, University Heart and Vascular Center, UKE Hamburg, Martinistraße 52, Hamburg 20246, Germany; [4]DZHK Standort Hamburg/Kiel/Luebeck, Martinistraße 52, Hamburg 20246, Germany; [5]Department of Cardiology, University Heart and Vascular Center, UKE Hamburg, Martinistraße 52, Hamburg 20246, Germany; [6]Division of Cardiovascular Medicine, Radcliffe Department of Medicine and British Heart Foundation Centre of Research Excellence Oxford, University of Oxford, Oxford, UK; [7]Medical Faculty, Core Facility Transgenic animal and genetic engineering Models (TRAM), University of Muenster, Muenster, Germany; and [8]Institute of Clinical Sciences, University of Birmingham, Birmingham, UK

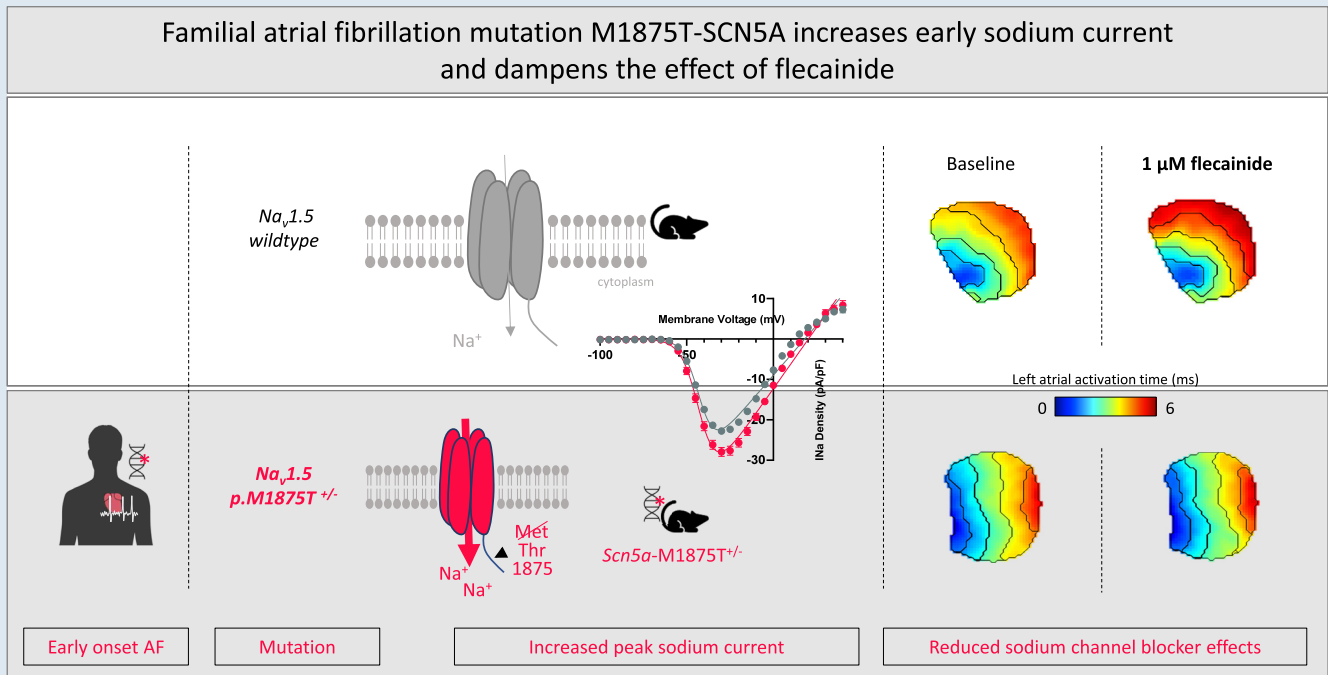|	
Aims	Atrial fibrillation (AF) is the most common cardiac arrhythmia. Pathogenic variants in genes encoding ion channels are associated with familial AF. The point mutation M1875T in the *SCN5A* gene, which encodes the α-subunit of the cardiac sodium channel Na$_v$1.5, has been associated with increased atrial excitability and familial AF in patients.
Methods and results	We designed a new murine model carrying the *Scn5a*-M1875T mutation enabling us to study the effects of the Na$_v$1.5 mutation in detail *in vivo* and *in vitro* using patch clamp and microelectrode recording of atrial cardiomyocytes, optical mapping, electrocardiogram, echocardiography, gravimetry, histology, and biochemistry. Atrial cardiomyocytes from newly generated adult *Scn5a*-M1875T$^{+/-}$ mice showed a selective increase in the early (peak) cardiac sodium current, larger action potential amplitude, and a faster peak upstroke velocity. Conduction slowing caused by the sodium channel blocker flecainide was less pronounced in *Scn5a*-M1875T$^{+/-}$ compared to wildtype atria. Overt hypertrophy or heart failure in *Scn5a*-M1875T$^{+/-}$ mice could be excluded.
Conclusion	The *Scn5a*-M1875T point mutation causes gain-of-function of the cardiac sodium channel. Our results suggest increased atrial peak sodium current as a potential trigger for increased atrial excitability.

* Corresponding author. Tel: +49 40 7410 57980. *E-mail address:* L.Fabritz@uke.de
† The first two authors contributed equally to the study.

Graphical Abstract

Familial atrial fibrillation mutation M1875T-SCN5A increases early sodium current and dampens the effect of flecainide

What's new?

- The point mutation M1875T in the C-terminal domain of the cardiac sodium channel Na$_v$1.5 causes an increase in early peak sodium current in atrial cardiomyocytes.
- The observed changes induced by this point mutation suggest an increase in peak sodium current as an electrophysiological substrate for the familial atrial fibrillation (AF) seen in patients.
- Our findings provide a possible explanation for the variable effectiveness of sodium channel blockers in patients with AF. Carriers of such sodium channel gain-of-function mutations may benefit more from tailored treatments.

Introduction

Atrial fibrillation (AF), the most common cardiac arrhythmia, is characterized by episodes of irregular and uncoordinated atrial electrical activity. It is associated with ischaemic stroke, cardiovascular death, and frequent hospitalizations.[1] A range of different common factors, such as heart failure, diabetes, and increased formation of fibrosis, can damage the atria.[2] These factors interact with a pre-existent, potentially inherited substrate to result in AF.[2] Inherited forms are characterized by early onset of the condition. Pathogenic variants in several genes associated with cardiomyopathies have been identified in familial AF, including variants in sarcomeric and cell-cell contact genes and others.[3] Within the group of ion channel genes, variants leading to dysfunction of the cardiac sodium channel (Na$_v$1.5) are associated with familial AF.[3,4] The pore-forming α-subunit of the Na$_v$1.5 is encoded by the SCN5A gene. Variants in SCN5A have been linked to several cardiac conditions, including AF.[4]

A missense SCN5A point mutation, Met1875Thr (M1875T), located in the C-terminus of the channel protein, was linked to autosomal dominant familial AF that spanned three generations.[5] Atrial ectopy was evident in mutation carriers in adolescence, and persistent AF occurred as early as 27 years of age. Analyses in the human cell line HEK293 heterologous expression system[5] suggested an enhanced function of the mutated Na$_v$1.5 channel.

To investigate the impact of the M1875T mutation in the heart and atria, we generated and characterized a novel knock-in murine model (Scn5a-M1875T$^{+/-}$). Mice that were heterozygous for the M1875T mutation were viable and studied herein. We investigated hearts of these mice from the whole organ in vivo to the level of the single cardiac cell ex vivo.

Methods

Generation and sequencing of the Scn5a-M1875T murine model

Mice heterozygous for the knock-in mutation M1875T in the Scn5a gene (Scn5a-M1875T$^{+/-}$) were generated by T-C point-mutating exon 28 of the cardiac sodium channel SCN5A gene using pSCN5a_targ3 targeting vector and CRISPR/Cas9 system in murine embryonic stem (ES) cells (Figure 1A). Mutation-harboring ES cells were characterized using Southern blot analysis and sequenced to exclude genomic rearrangements (Figure 1B),[6] and injected into B6D2F1 mouse blastocysts. Sequencing analysis of the mutation-containing region using DNA from adult wildtype (WT) and heterozygous Scn5a-M1875T$^{+/-}$ mice on C57Bl/6J × 129sv hybrid genetic background are shown in Figure 1C. Detailed steps of the generation are further explained in the supplement.

Methionine at position 1875 of the human Na$_v$1.5 protein sequence corresponds to position 1877 of the murine sequence. The latter is therefore point-mutated in this model. However, to underpin the bedside-to-bench
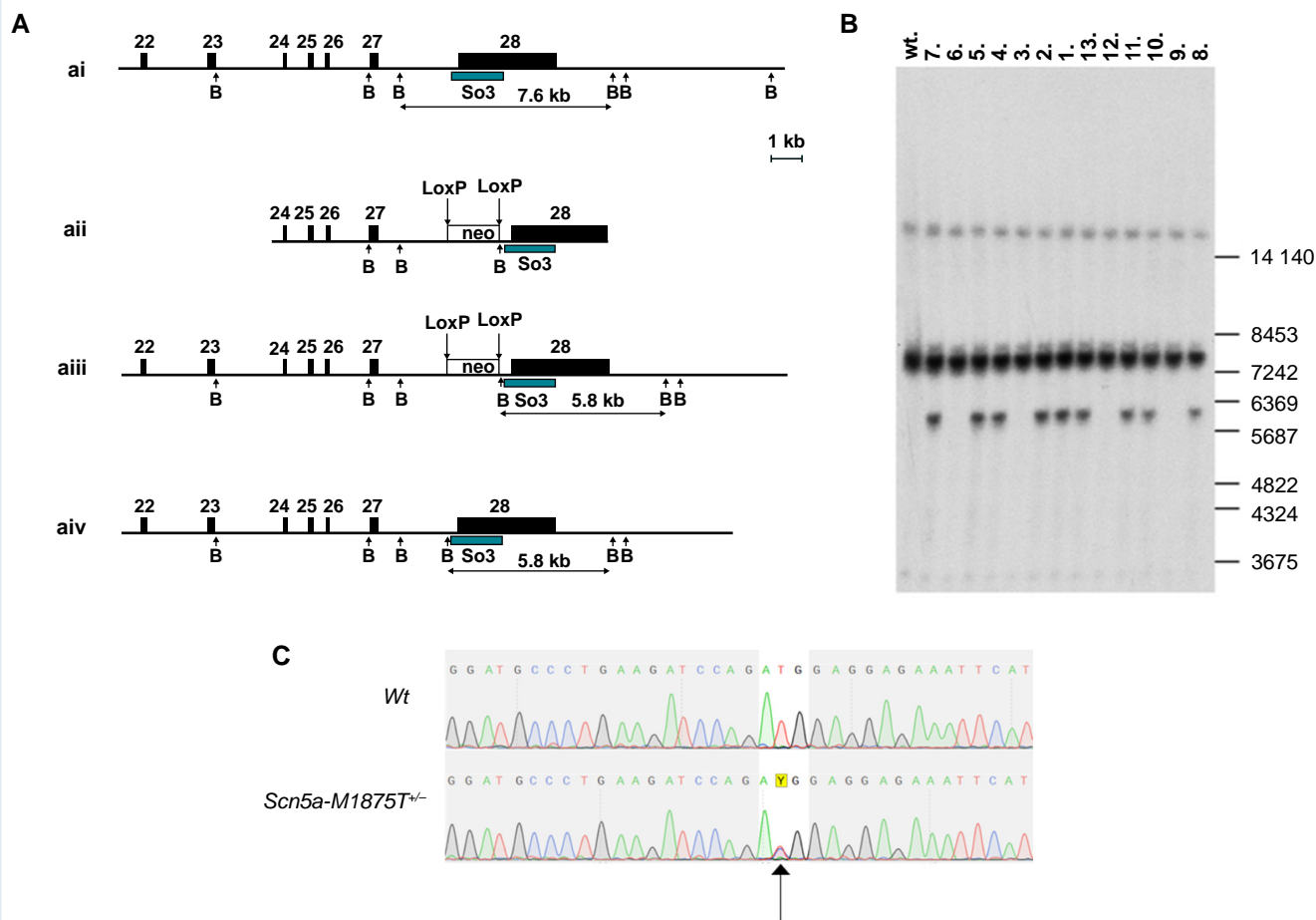
Figure 1 Targeting of exon 28 of the mouse *Scn5a* gene in order to introduce the M1875T coding mutation and sequencing confirmation of its presence. (*A*) The intronic and intergenic regions are shown as lines, and exons are shown as filled boxes. The empty box corresponds to the neomycin resistance cassette (neo) flanked by the Locus of x-over, P1 (LoxP) sites (vertical arrows). Exon numeration is shown above. The arrows below are corresponding to Bacillus amyloli (BamHI) restriction endonuclease sites (*B*). The black box corresponds to Southern probe sequences (So3). The expected sizes of restriction DNA fragments are indicated below in kb. (*AI*) Wildtype (WT) locus. (*AII*) Targeted vector structure (without negative selection marker and plasmid backbone). (*AIII*) Genomic locus after the homologous recombination. The neomycin cassette is present in intron 27 and flanked by two LoxP sites. (*AIV*) Genomic locus after the Cyclic recombinase-mediated neo cassette deletion. (*B*) Southern blot analysis of DNA isolated from mouse tail biopsy of the F1 offspring (1–13) and hybridized with the So3 probe. With help of the BamHI enzymatic digestion, we detect the WT allele 7.6 kb and targeted allele 5.8 kb. DNA samples 1, 2, 4, 5, 7, 8, 10, 11, and 13 contain correctly targeted *Scn5a* gene (Scn5a-M1875T$^{+/-}$). Positions of the size marker (in bp) are shown on the right. The WT control animal is labeled 'wt'. (*c*) Sequencing analysis of the *Scn5a* gene region containing the mutation site in back-crossed adult mice (on pure genetic background). The T-C mutation on one allele causing the methionine-threonine exchange at position 1875 (1877) is indicated by an arrow.

nature of this investigation, we use the human annotation and refer to it as 'Scn5a-M187**5**T' throughout this manuscript.

Mice were bred on an FVB or 129/sv genetic background and housed in individually ventilated cages with sex-matched littermates (2–5 mice/cage), under standard conditions: 12 h light/dark circle, 22°C and 55% humidity. Food and water were available *ad libitum*. The health status of mice used in the study was monitored daily and prior to experiments.

Functional experiments were conducted on hearts of male and female young adult mice of pure background (8–20 weeks), heterozygous for the knock-in mutation M1875T in the *Scn5a* gene (*Scn5a*-M1875T$^{+/-}$) and their WT littermates. Mice of both sexes and background were used evenly and analysed jointly, to make the data more widely applicable.

Study approval

All procedures were performed in compliance with the guidelines from Directive 2010/63/EU of the European Parliament on the protection of animals used for scientific purposes and conducted in accordance with rules and regulations for experiments with animals and approved by the UK Home Office (PPL number 30/2967) and by the institutional review board of University of Birmingham.

Electrocardiogram recordings *in vivo*

Non-invasive electrocardiograms (ECGs) were recorded in conscious young adult mice (8–19 weeks) using a tunnel system for gentle restraint (ecgTunnel, EMKA Technologies, Paris, France).[7] ECG recordings were analysed using ECGauto software (EMKA Technologies, Paris, France). ECGs were also recorded in isoflurane-sedated mice during echocardiography as below.

Echocardiography *in vivo*

Echocardiography was performed in sedated mice (0.5–2% isoflurane, supplemented with 100% O$_2$) using Vevo® 2100 system (VisualSonics, Amsterdam,

Netherlands) as reported previously.[8] Heart rate was maintained at 450 ± 70 bpm. Left atria (LA) were visualized in the parasternal long axis view in the plane of the aortic root. LA area and diameter were measured during pre-atrial contraction, using the P-wave of the limb ECG trace as a guide.

Histological analysis

Hearts were fixed in formalin and paraffin-embedded tissues were cut into slices of 4 µm. Sections were dewaxed, stained with hematoxylin and eosin for overviews and subsequently dehydrated, embedded and imaged on a NanoZoomer 2.0-HAT (Hamamatsu).

Slides used for quantitative analysis were cooked in citrate buffer for antigen retrieval. Autofluorescence was quenched with a 0.25% Sudan black solution for 30 min and samples were blocked with 2% Bovine serum albumin (BSA)/ 2.2% Glycine for 1 h at room temperature (RT). Wheat germ agglutinin (WGA) with Alexa Fluor™ 488 Conjugate (1:200, W11261, Invitrogen) was applied for 2 h at RT.

Images of WGA-stained cardiac tissue were obtained with a confocal microscope equipped with an Aurox Clarity (Aurox Ltd.) spinning disc unit and a $20\times$ EC Plan-Neofluar objective (420353-9900-000, Zeiss, NA = 0.5) run with Aurox Visionary (Aurox Ltd.) software.

Quantitative analysis of WGA-stained area and cardiac cell diameters as shown in *Figure 2* was carried out using a published ImageJ plugin for atrial histological analysis (JavaCyte[9]), with minor adjustments.

Atrial cardiomyocyte isolation

Murine hearts were excised under deep terminal anaesthesia (4% isoflurane inhalation in O_2, 1.5 L/min) and perfused at 4 mL.min⁻¹ at 37°C on a vertical Langendorff apparatus with the following solutions, equilibrated with 100% O_2: (i) N-2-hydroxyethylpiperazine-N-2-ethane sulfonic acid (HEPES)-buffered, Ca^{2+}-free, modified Tyrode's solution containing in mM: NaCl 145, KCl 5.4, $MgSO_4$ 0.83, Na_2HPO_4 0.33, HEPES 5, and glucose 11 (pH 7.4, NaOH)×5 min and (ii) Tyrode's enzyme solution containing 640 µg/mL collagenase type II (270 U/mg), 600 µg/mL collagenase type IV (270 U/mg) and 50 µg/mL protease (Worthington, Lakewood, NJ), 20 mM taurine and 3 µM $CaCl_2 \times 8$–12 min.[10] The heart was removed from the Langendorff setup and perfused with 5 mL of modified Kraftbruhe (KB) solution containing in mM: DL-potassium aspartate 10, L-potassium glutamate 100, KCl 25, KH_2PO_4 10, $MgSO_4$ 2, taurine 20, creatine 5, Ethyleneglycol- bis(β-aminoethyl)-N,N,N☐,N☐-tetraacetic Acid (EGTA) 0.5, HEPES 5, 0.1% BSA, and glucose 20 (pH 7.2, KOH).

The LA was dissected free and cardiomyocytes were dissociated gently with fire-polished glass pipettes (2 to 1 mm diameter in sequence). Cells were re-suspended in 2 mL KB buffer and Ca^{2+} was gradually reintroduced to the cell suspension incrementally over a period of 2 h to reach a final concentration of 1 mM. All experiments were performed within 8 h of isolation.

Whole-cell patch clamp electrophysiology of isolated atrial cardiomyocytes

Dissociated murine LA cardiomyocytes were plated on, and allowed to adhere to, laminin-coated coverslips (10 mm diameter) for at least 20 min. Coverslips were transferred to a recording chamber and were continually superfused at 3 mL.min⁻¹, with a low Na^+ external solution containing in mM; NaCl 10, KCl 4.5, $C_5H_{14}CINO$ 130, $CaCl_2$ 1, $MgCl_2$ 1.2, HEPES 10 and glucose 10 (pH 7.4 with CsOH). To block L-type Ca^{2+} currents, 2 mM $NiCl_2$ was added to the superfusate. Experiments were performed at 22 ± 0.5°C. Whole-cell patch clamp recordings were obtained in voltage-clamp mode using borosilicate glass pipettes (tip resistances 1.5–3 MΩ).

For Na^+ current recordings, the pipette solution contained in mM: CsCl 115, NaCl 5, EGTA 10, HEPES 10, MgATP 5, Tetraethylammonium Chloride (TEACl) 20 and $MgCl_2$ 0.5 (pH 7.2, KOH). Voltage-dependent Na^+ currents were evoked by 5 mV step depolarizations (100 ms) from a holding potential of −100 mV to test potentials ranging from −95 mV to +40 mV. Cells were excluded from analysis if there was no reversal of the sodium current by +40 mV. To investigate Na_v1.5 voltage-dependent inactivation kinetics, cells were subject to 500 ms pre-pulses ranging from −120 mV to −40 mV, followed by a 100 ms step to −30 mV. For Na_v1.5 time-dependent recovery kinetics, a standard two pulse protocol was used (−120 mV to −30 mV, 20 ms), with the time between the two pulses incrementally varying between 5 and 950 ms.

All recordings and analysis protocols were performed using an Axopatch 200B amplifier (Molecular Devices, USA) and digitized at 50 kHz using a CED micro1401 driven by Signal v6 software (Cambridge Electronic Design, Cambridge, UK). Series resistance was compensated, ranging between 60–100% for all cells. Experiments were terminated if series resistance abruptly changed or was above 10 MΩ.

Atrial microelectrode recordings

As previously described,[11,12] following isolation the LA was immediately transferred into a dissecting chamber and continuously superfused at 10 mL.min⁻¹ with a bicarbonate buffered Krebs-Henseleit (KH) solution containing in mM: NaCl 118; $NaHCO_3$ 24.88; KH_2PO_4 1.18; Glucose 11; $MgSO_4$ 0.83; $CaCl_2$ 1.8; KCl 3.52, equilibrated with 95% O_2/5% CO_2, 36–37°C, pH 7.4. Micro-dissection and pinning out of the LA was performed using a dissection microscope (Stemi SV 11, Zeiss, Germany). The LA was paced at 1–10 Hz via bipolar platinum electrodes. Action potentials (APs) were recorded from freely contracting LA using custom made glass floating microelectrodes containing 3 M KCl, (resistance 15–30 MΩ). Voltage signals were amplified and digitized at 20 kHz and were unfiltered (Axoclamp 2B; Molecular Devices, California, USA; Spike2 software Cambridge Electronic Design, Cambridge, UK). Measured parameters included the resting membrane potential (RMP), AP amplitude (APA), peak depolarization rate (dV/dt), and AP duration (APD) at 30–90% repolarization. APs were only analysed following sufficient rate adaptation achieved after at least 50 stimulated APs at each frequency.

Atrial optical mapping

Optical mapping of the LA was conducted as previously described.[13] Isolated whole hearts were loaded on to a vertical Langendorff apparatus and perfused with a standard KH solution. Hearts were perfused at 4 mL.min⁻¹ (equilibrated with 95%O_2/5%CO_2 and heated to 36–37°C, pH 7.4). Hearts were loaded with 25 µL of voltage sensitive dye Di-4-ANEPPS at a concentration of 5 mg/mL, diluted in 1 mL of KH solution and delivered via bolus port injection over 3–5 min. The LA was then isolated and pinned in a superfusion chamber containing 37°C KH solution for transfer to the optical mapping setup, anterior surface facing up.

In the optical mapping system, atria were superfused with KH solution (95%O_2/5%CO_2, 36–37°C) containing contraction uncoupler Blebbistatin (35 µM). For imaging, atria were illuminated by two dual LEDs at 530 nm. A 630 nm long-pass filter was used to separate emitted fluorescence, imaged using an ORCA flash 4.0 CMOS camera (Hamamatsu, Japan). Images were acquired at a framerate 0.987 kHz and pixel size of 71 µm/pixel.[2] Atria were paced using bipolar platinum electrodes delivering 2 ms pulses at twice diastolic threshold (minimum voltage required to elicit APs).

One-minute baseline recording was taken following a 10 min equilibration period to ensure contraction uncoupling and temperature re-stabilization. During imaging, atria were initially paced at 330 ms pacing cycle length (PCL). A 'ramp' pacing protocol was then initiated, in which the atria were paced at 120 ms PCL for 100 stimuli and then PCL was reduced from 120 ms to 80 ms in 10 ms intervals every 20 stimuli. After taking baseline recordings, LED illumination was switched off and the superfusion solution replaced with an identical solution containing flecainide, a clinically-used sodium channel blocker[14] at a concentration of 1 µM and then 5 µM (or control solution without flecainide for time control experiments).

Subsequent recordings were then made as described above after 20 min superfusion with 1 µM flecainide solution and then further 15 min with 5 µM flecainide solution. Atria were paced at 330 ms PCL continuously in dark conditions between recordings.

From these recordings, APD and conduction velocity (CV) were mapped across the LA using ElectroMap software.[13] Atria were removed from analysis at a given PCL if loss of 1:1 capture ratio with pacing stimuli (i.e. missed beats) was observed.

Statistics

For all murine experiments presented herein, experimenters were blinded to the genotype of the littermate pairs during data collection and analysis. Student's *t*-tests were used for singular comparisons for normally distributed data. A hierarchical nested *t*-test (*Figure 3*) and Mann–Whitney test (see Supplementary material online, *Table S3*) were used where appropriate.
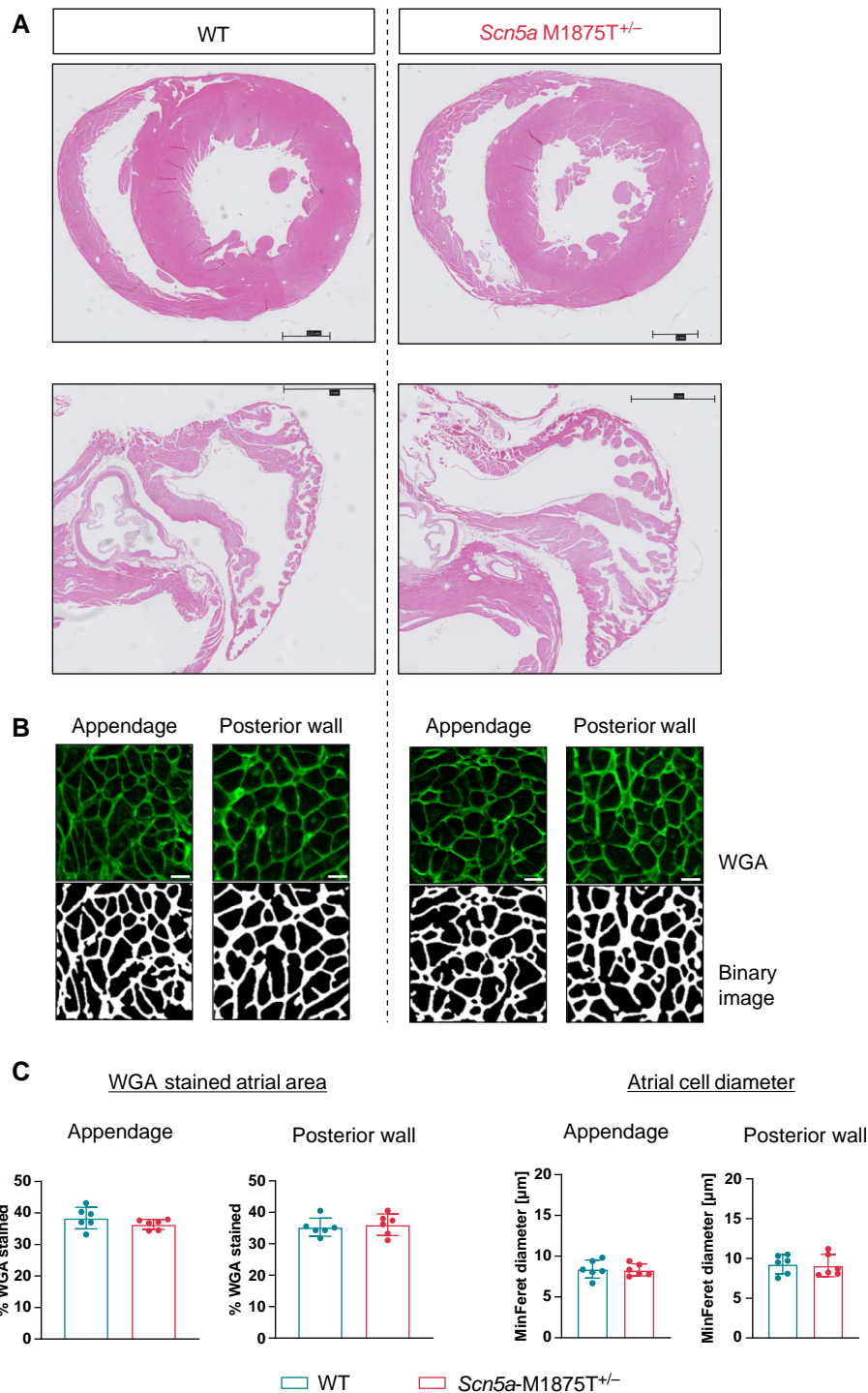
Figure 2 Unaltered atrial amount of extracellular matrix content and myocyte diameter. (*A*) Hematoxylin and eosin-stained sections of wildtype (WT) and *Scn5a*-M1875T[+/−] litter pair hearts (ventricles, upper panel; left atria, lower panel). Scale bars represent 1 mm. There were no obvious differences between genotypes. (*B*) Exemplary immunofluorescence images from atrial regions of interest (ROI) of wheat germ agglutinin (WGA) staining and corresponding binary images for quantification in left atrial (LA) appendage and LA posterior wall from WT and *Scn5a*-M1875T[+/−] hearts. Scale bars represent 10 μm. (*C*) Quantification of WGA-stained atrial area and atrial cell diameters from transverse sections as depicted in (*B*). Neither parameter was affected by the point mutation (WGA-stained atrial area quantified from LA appendage: $n = 6$ hearts and 65/67 individual ROI per group; LA posterior wall $n = 6$ hearts and 26/29 ROI per group. Atrial cell diameter quantified from LA appendage: $n = 6$ hearts and 14 563/13 368 individual cells per group; LA posterior wall and 8283/8384 individual cells per group). Data are presented as mean ± SD.

Figure 3 Isolated atrial cardiomyocytes with the *Scn5a*-M1875T$^{+/-}$ mutation have a larger sodium current than wildtypes when measured with whole-cell patch clamp electrophysiology. (*A*) Representative sodium current (I$_{Na}$) traces from whole-cell voltage clamp recording of isolated left atrial (LA) cardiomyocytes from wildtype (WT) (left, dark turquoise) and *Scn5a*-M1875T$^{+/-}$ (light red, right) hearts. (*B*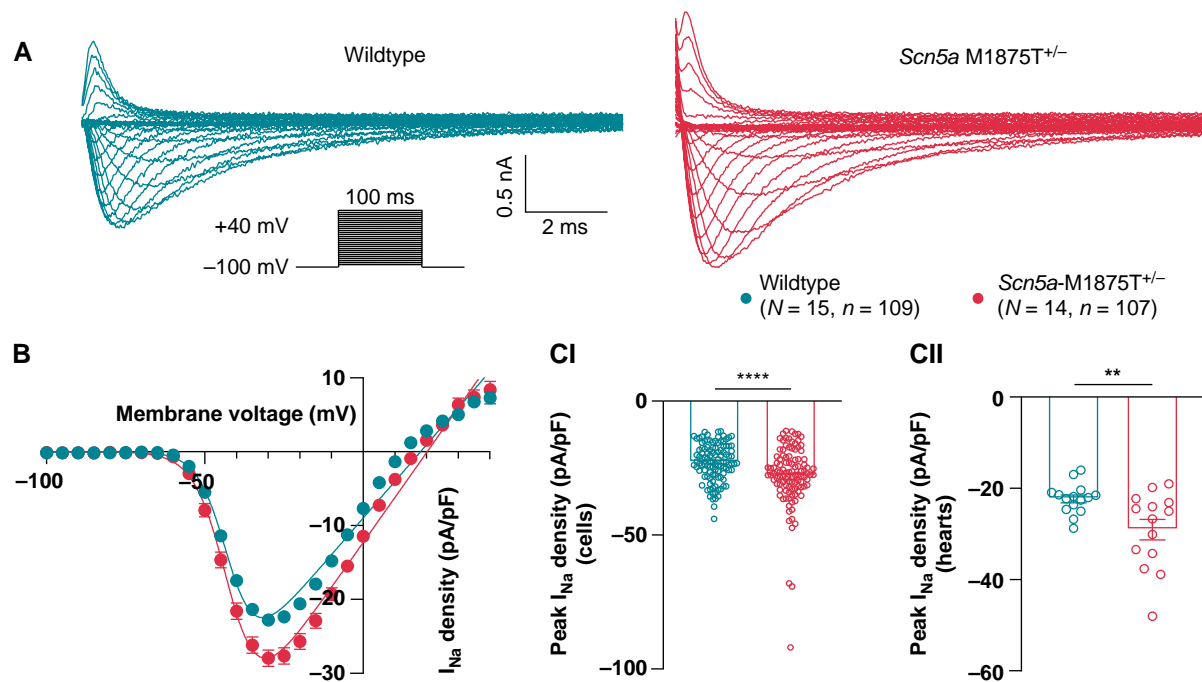) Normalized grouped data revealed that the *Scn5a*-M1875T$^{+/-}$ mutation increases peak I$_{Na}$ in LA cardiomyocytes over test potentials ranging from −100 to +40 mV. (*C*) At the peak I$_{Na}$ test potential of −30 mV, *Scn5a*-M1875T$^{+/-}$ cardiomyocytes had a significantly larger I$_{Na}$ than WTs, both when comparing individual cells (*n* = 109 WT, *n* = 107 *Scn5a*-M1875T$^{+/-}$) (*CI*) and hearts (*n* = 15 WT, *n* = 14 *Scn5a*-M1875T$^{+/-}$) (*CII*). Data are presented as the mean ± SEM.

Multiple comparisons were made using two-way ANOVA with Bonferroni's post-hoc tests. For current–voltage graphs (*Figure 3B*), a Boltzmann curve was fit to the data, using the modified Boltzmann equation: I$_{Na}$ = G$_{max}$(V$_m$ − V$_{rev}$)/(1 + Exp[(V$_{0.5}$-V$_m$)/k]), where I$_{Na}$ is the current density at an equivalent test potential (V$_m$), G$_{max}$ is the peak conductance (nS), V$_{rev}$ is the reverse potential, V$_{0.5}$ is the membrane potential at 50% current activation, and k is the slope constant. All graphical representations display individual measurements. Means are quoted and shown in Figures ± SEM unless stated otherwise. Level of statistical significance is shown in Figures as follows: *$P < 0.05$; **$P < 0.01$; ***$P < 0.001$; ****$P < 0.0001$. Statistics and Figures were created using Prism 8 (GraphPad Software, San Diego, California).

Results

Viable heterozygous *Scn5a*-M1875T$^{+/-}$ mice show normal cardiac size, structure, and basic function

The point mutation previously identified in patients with early familial AF was successfully introduced to exon 28 of the mouse *Scn5a* gene via homologous recombination of a targeting vector. The vector contained the T-C point mutation (CRISPR/cas9-mediated) resulting in methionine-threonine exchange in the Na$_v$1.5 protein (*Figure 1*; see Supplementary material online, *Figure S1A*). Offspring from both WT × heterozygote (=*Scn5a*-M1875T$^{+/-}$) and heterozygote × heterozygote pairings were viable. No homozygous *Scn5a*-M1875T$^{-/-}$ offspring were born (see Supplementary material online, *Figure S1B*), suggesting embryonic lethality, as previously reported for other *Scn5a* mutations.[15] Accordingly, the ratio of WT and heterozygous animals shifted from 1:2 (expected) to approximately 1:3 when heterozygous animals

were crossed (see Supplementary material online, *Figure S1B*). The ratio of male:female sex in offspring approximated 1:1 as expected (see Supplementary material online, *Figure S1C*).

Age-matched young adult WT and *Scn5a*-M1875T$^{+/-}$ mice displayed similar heart rate, PR-, QRS- and QT- interval in ECGs recorded awake (see Supplementary material online, *Table S1*) and during sedation (see Supplementary material online, *Table S2*). Echocardiography and histological examination excluded overt differences in structure (see Supplementary material online, *Table S3*; *Figure 2A*). Neither atrial extracellular matrix content nor atrial cardiomyocyte cell diameter were affected by the mutation (*Figure 2B and C*; see Supplementary material online, *Figure S2A*). Accordingly, pro atrial natriuretic peptide protein expression (proANP) was detected in right atria as expected but was not elevated in ventricles (see Supplementary material online, *Figure S2B*).

Atrial *Scn5a*-M1875T$^{+/-}$ cardiomyocytes have an augmented peak sodium current density

To determine the impact of the M1875T point mutation on peak I$_{Na}$ amplitude and Na$_v$1.5 channel gating properties, left atrial cardiomyocytes from WT and *Scn5a*-M1875T$^{+/-}$ mice (8–13 weeks) were isolated and whole-cell patch clamp recordings were performed.

The M1875T variant increased I$_{Na}$ over test potentials ranging from −100 to +40 mV (*Figure 3A and B*). At a peak test potential of −30 mV, mean left atrial cardiomyocyte I$_{Na}$ density was higher in *Scn5a*-M1875T$^{+/-}$ (−28.0 ± 1.1 pA/pF, *n* = 107 cells) than in WT littermates (−22.8 ± 0.7 pA/pF, *n* = 109 cells, $P < 0.0001$; *Figure 3C*). The elevation in I$_{Na}$ was also apparent when recordings were grouped by heart
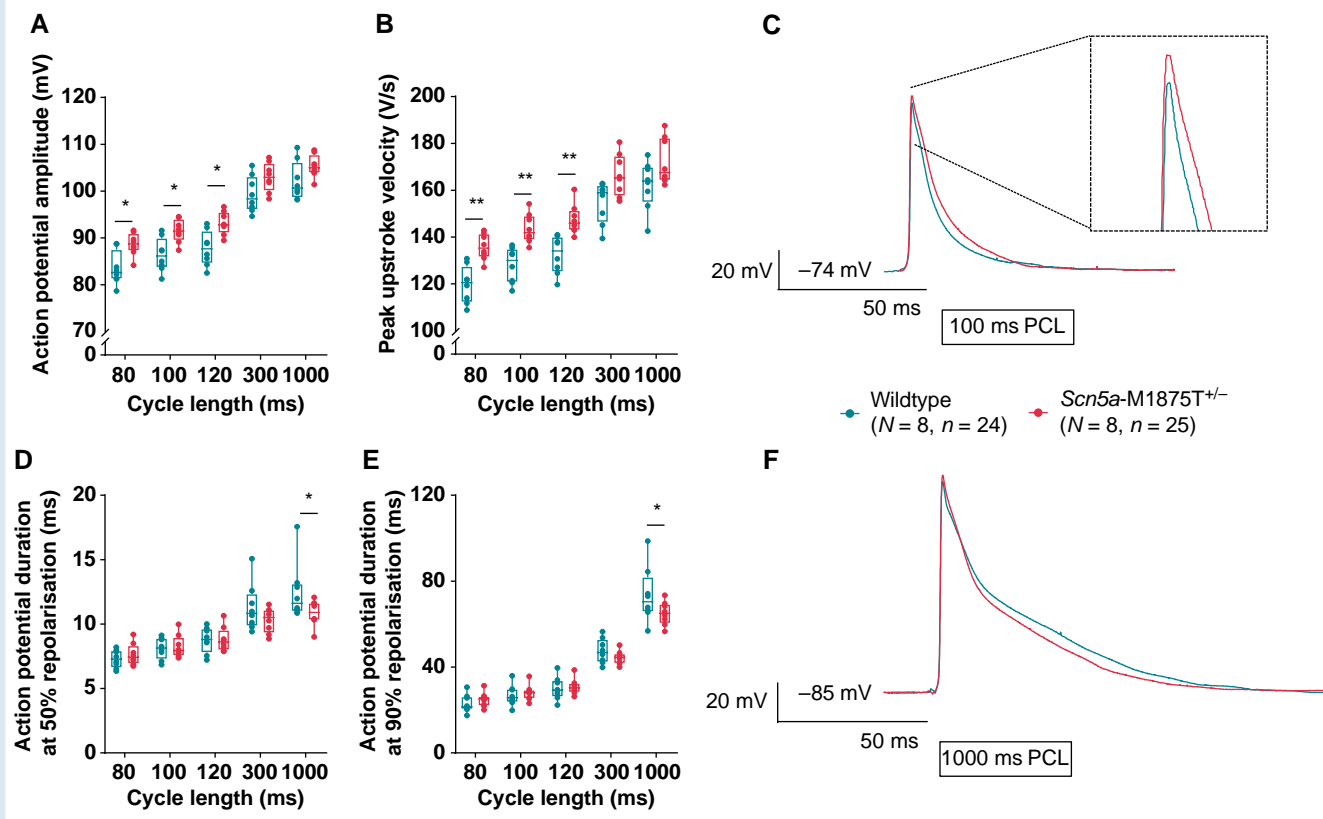
Figure 4 Action potentials from atria with the *Scn5a*-M1875T$^{+/-}$ mutation have a larger action potential amplitude and a faster peak upstroke velocity when measured with the sharp microelectrode technique. (*A*) *Scn5a*-M1875T$^{+/-}$ left atria (LA) had a significantly larger action potential (AP) amplitude at shorter pacing cycle lengths (PCLs) of 80–120 ms (*P* < 0.05) and (*B*) a significantly faster peak upstroke velocity (dV/dt). (*C*) Representative AP traces from WT (dark turquoise) and *Scn5a*-M1875T$^{+/-}$ (light red) LA stimulated at 100 ms PCL. (*D–F*) When paced at 1000 ms PCL, *Scn5a*-M1875T$^{+/-}$ LA had a significantly shorter AP duration (APD) when measured at 50% (APD50) (*D*) and 90% (APD90) (*E*) repolarisation. *P < 0.05, **P < 0.01, wildtype (WT) vs. *Scn5a*-M1875T$^{+/-}$, *n* = 8 per group, *n* = 24 WT, *n* = 25 *Scn5a*-M1875T$^{+/-}$; ANOVA statistics. (*F*) Representative AP traces from WT (dark turquoise) and *Scn5a*-M1875T$^{+/-}$ (light red) LA stimulated at 1000 ms PCL. Data in (*A*), (*B*), (*D*), and (*E*) are presented as box-whiskers with box limits denoting the interquartile range (IQR) and the whiskers projecting to the outliers.

(*Scn5a*-M1875T$^{+/-}$ −29.1 ± 2.2 pA/pF, *n* = 14 vs. WT −22.3 ± 0.9 pA/pF, *n* = 15, *P* = 0.0075; *Figure 3C*) and after applying hierarchical analysis (*Scn5a*-M1875T$^{+/-}$ −29.1 ± 1.1 pA/pF, *n* = 107 cells, *n* = 14 mice vs. WT −22.3 ± 0.9 pA/pF, *n* = 109 cells, *n* = 15 mice, *P* = 0.0093).

Capacitance measurements were not different between genotypes, indicative of similar cell size of atrial cardiomyocytes (see Supplementary material online, *Figure S3A*).

Whole-cell I_{Na} voltage-dependent inactivation and time-dependent recovery kinetics were not altered in *Scn5a*-M1875T$^{+/-}$ cardiomyocytes compared to WT (see Supplementary material online, *Figure S3B and C*). Na$_v$1.5 expression in hearts of *Scn5a*-M1875T$^{+/-}$ mice at the mRNA and the protein level revealed no difference at either the whole cell or isolated membrane fraction level (see Supplementary material online, *Figure S4*).

APs from *Scn5a*-M1875T$^{+/-}$ atria have a larger amplitude and faster peak upstroke velocity

APs were measured in whole left atrial tissue isolated from WT and *Scn5a*-M1875T$^{+/-}$ mice (9–13 weeks) using sharp microelectrodes.

APA was significantly larger in *Scn5a*-M1875T$^{+/-}$ murine left atria at all PCLs tested and this effect was more pronounced at shorter cycle lengths (*n* = 8, *n* = 24–25; *Figure 4A*). The variant resulted in a faster peak upstroke

velocity (dV/dt), especially at the shorter cycle lengths (100 ms PCL: WT 128.0 ± 3.3, *n* = 24; *Scn5a*-M1875T$^{+/-}$ 142.8 ± 4.0 mV/ms, *n* = 25, *P* = 0.0282; *Figure 4B*, representative traces *Figure 4C*).

The RMP was not different between genotypes (100 ms PCL: WT −72.4 ± 0.6; *Scn5a*-M1875T$^{+/-}$ −73.1 ± 0.6 mV). Atrial activation times were also similar (100 ms PCL: WT 4.9 ± 0.2; *Scn5a*-M1875T+/− 4.9 ± 0.2 ms) (see Supplementary material online, *Table S4*). Only at the long PCL of 1000 ms, the APD at 50 and 90% repolarization was shorter in *Scn5a*-M1875T$^{+/-}$ left atria than in WT (*Figure 4D–F*), while the APD at 30% and 70% repolarization was not significantly different (see Supplementary material online, *Table S4*). Similarly, optical mapping data showed no APD differences at PCLs tested. We performed analyses of APD restitution (see Supplementary material online, *Figure S5*), which suggest that an effect of the M1875T mutation may be a blunting of APD restitution.

Flecainide-induced atrial conduction slowing and post-repolarization refractoriness is less pronounced in *Scn5a*-M1875T$^{+/-}$ atria

Optical mapping of WT and *Scn5a*-M1875T$^{+/-}$ whole left atrial tissue was performed to test effects of the heterozygous *Scn5a*-M1875T

Figure 5 The response to the anti-arrhythmic agent flecainide is reduced in Scn5a-M1875T[+/−] atria in optical mapping. (A) Example left atrial (LA) activation maps from wildtype (WT, top panels) and Scn5a-M1875T[+/−] (bottom panels) mice. Left panels show activation at baseline, right panels show activation of the same atria following exposure to 1 µM flecainide for 20 min. (B) Grouped data showing change in conduction velocity (ΔCV) following exposure to 1 µM flecainide in WT (dark turquoise) and Scn5a-M1875T[+/−] (light red) LA for 20 min at different pacing cycle lengths. (C) Example traces of optical action potentials (APs) recorded following further treatment of WT (top, dark turquoise) and Scn5a-M1875T[+/−] (bottom, light red) LA with 5 µM flecainide for 15 min while reducing pacing cycle length (increasing pacing frequency). (D) Grouped data showing minimum pacing frequency in beats per minute (bpm) at which 1:1 stimulus capture was maintained in WT (dark turquoise) and Scn5a-M1875T[+/−] (light red) LA following exposure to 5 µM flecainide. Time control data (green) shows minimum PCL at which 1:1 stimulus capture was maintained in atria that were not exposed to flecainide but had been under experiment conditions for the same time period (35 min from baseline recording). $n = 12$ per group at 330–100 ms PCL. Atria were excluded from further analysis at shorter PCLs if 1:1 capture was lost, only data in steady state was used. $n = 5$ for time control experiments. *$P < 0.05$, **$P < 0.01$, WT vs. Scn5a-M1875T[+/−]; ANOVA statistics. Data are represented as box-whiskers with box limits denoting the interquartile range (IQR) and the whiskers projecting to min and max values (B) or as the mean ± SEM (D).

mutation on atrial conduction. Left atria were superfused with the open channel sodium channel blocker flecainide (1 µM, clinically used concentration) to determine the response of Scn5a-M1875T[+/−] and WT left atria. While CV was unchanged at baseline, flecainide slowed conduction less in Scn5a-M1875T[+/−] left atria (CV difference at 100 ms PCL −6 ± 1 cm/s, $n = 12$, $P = 0.0357$) than in WTs (CV difference at 100 ms PCL −10 ± 1 cm/s, $n = 12$, $P = 0.0357$; Figure 5A and B; see Supplementary material online, Figure S6).

We also investigated flecainide-induced changes in left atrial refractoriness as it is known that flecainide induces post-repolarization refractoriness using rapid atrial pacing. Representative optical AP recordings show 1:1 capture in the Scn5a-M1875T[+/−] left atria with flecainide, while several stimuli in the WT left atria did not elicit APs (Figure 5C). All time-controlled left atria (no flecainide, same experimental duration) were successfully paced with 1:1 capture down to 80 ms PCL. Loss of 1:1 capture began at longer PCLs in WT (7/12 atria lost 1:1 capture at PCLs ≤ 120 ms, Figure 5D) compared to Scn5a-M1875T[+/−] (1/12 atria lost 1:1 capture at PCLs ≤ 120 ms, $P =$

0.0185) left atria. The diastolic pacing threshold remained consistent throughout experiments. Thus, flecainide induced less pronounced post-repolarization refractoriness in the Scn5a-M1875T[+/−] left atria.

Discussion

Main findings

Our study describes the effects of the familial AF mutation Scn5a-M1875T[+/−] in a newly generated murine model. Key findings are that the M1875T Scn5a mutation leads to an increased atrial AP upstroke velocity and amplitude, and a selective increase in the early cardiac sodium current (I_{Na}). Atrial cardiomyocyte capacitance and size, as well as cardiac size and function, are preserved. The effect of the sodium channel blocker flecainide is dampened in Scn5a-M1875T[+/−] atria. Our measurements in this new murine model confirm that a selective increase of I_{Na} may lead to familial AF as observed in the family affected,

and suggest that commonly used concentrations of sodium channel blockers may be less effective in familial forms of AF with a selective increase in I_{Na} than in other types.

Gain-of-function properties of *Scn5a*-M1875T$^{+/-}$ sodium channels in the murine atrium

Our data show a gain-of-function variant, namely an increased early sodium current as evidenced by an augmented APA and upstroke velocity, and larger I_{Na} in hearts with a *Scn5a*-M1875T$^{+/-}$ variant.

In contrast to findings in HEK293 cells,[5] there was no depolarizing shift of $Na_v1.5$ channel inactivation in murine left atrial cardiomyocytes observed. Instead, we show a similarly augmented I_{Na} without alterations in channel gating properties. Generation of the murine mutant model allowed us to study mutated sodium channels in cardiac tissue within the presence of the greater protein complex including α- and β-subunits and other membrane proteins, a complete cardiomyocyte contractile apparatus and all other cardiac cell types.

SCN5A genetic variants reported show various underlying mechanisms mainly linked to channel dysfunction, defective channel trafficking, or protein complex formation.[16] Cardiac sodium channels have been observed to form dimers and different regions of the channel protein have been implicated in dimerization.[17] Structural analysis following the hypothesis of $Na_v1.5$ dimerization via C-terminal interaction reveals that the surface of residue Met1875 of one $Na_v1.5$ cytosolic C-terminus will interact with Ala1924 of a second $Na_v1.5$.[17] This prediction suggests that the location site containing the mutation in our model could provide a structural basis for altered $Na_v1.5$-$Na_v1.5$ channel interaction further to be investigated.

It is unlikely that the M1875T mutation increases the *late* sodium current ($I_{Na, l}$), as APs we measured were not prolonged by the mutation, in line with the initial report of the mutation in human embryonic kidney (HEK) cells.[5] A lack of AP prolongation clearly differs to findings in the gain-of-function mutation *ΔKPQ-Scn5a*$^{+/-}$ mutant murine model which shows an increase in $I_{Na,l}$[11] with prolonged atrial and ventricular APD, especially at longer PCLs. This suggests that the M1875T mutation acts differently to, and is distinct from, *SCN5A* gain-of-function mutations leading to prolonged repolarization and long QT syndrome, in concordance with the broad spectrum of phenotypic outcomes resulting from mutations in the same ion channel gene.[18]

It could be of interest to model the effects of the increased I_{Na} including effects on restitution and on human atrial AP models, e.g. higher amplitude and upstroke velocity at fast rates, while a slight APD shortening was only seen at slower rates.

Effect of *Scn5a*-M1875T$^{+/-}$ on conduction and refractoriness

While defects in the cardiac sodium channel can also cause conduction disturbances,[16,18] this variant shows a dampened response to flecainide both on conduction and post-repolarization refractoriness. Flecainide is a clinically used sodium channel blocker that inhibits cardiac I_{Na} via blocking the pores of open $Na_v1.5$ channels.[10,14] The differential response to flecainide is likely due to the increased early sodium influx through the mutated $Na_v1.5$ channels, enabling preservation of conduction and activation properties in atrial cardiomyocytes when sodium channels are inhibited, leading to an enhanced activation reserve.

Limitations

This study primarily investigated which alteration in sodium channels is the basis for the clinically observed AF in the family carrying the mutation. Spontaneous AF was not observed during the single time point ECG. Detailed investigation of the arrhythmia trigger and

pro-arrhythmic effects in the model, e.g. using telemetry and electrophysiological studies, are warranted in the future. It would also be of interest to systematically investigate the effect of the mutation on ventricular I_{Na}.

Murine models have limitations due to differences between mice and human, but due to consistency in sodium currents have been useful in characterizing sodium channel mutations.[8,11,15] Identified mutation-induced changes at the cellular and organ level in this model appear sufficient to explain AF in the original family. Studies in human cardiomyocytes and in atrial engineered heart tissue would be desirable to assess the effect of the M1875T mutation in human models in the future.

Conclusion

The *Scn5a*-M1875T$^{+/-}$ variant causes a selective increase in the early cardiac sodium current, leading to an increased activation reserve and reduced refractoriness, whilst structure and contractile function are preserved. These findings can explain the familial occurrence of atrial ectopy and AF in the absence of reported severe heart disease. More widely they suggest a mechanism by which altered cardiomyocyte sodium current can predispose to AF. Our data also show that the M1875T gain-of-function mutation decreases the effectiveness of sodium channel blockers such as flecainide, which may have implications for treatment.

Supplementary material

Supplementary material is available at *Europace* online.

Authors' contributions

L.F. and P.K. designed the research; BVS generated the mouse model in TRAM upon request by P.K. and L.F.; M.O., L.C.S., C.O., S.B.S., S.A., J.S.R., S.N.K., A.M., D.D., L.Fo., L.F., and A.P.H. conducted experiments, analysed data, and performed statistical analysis; K.G., D.P., A.P.H., P.K., and L.F. supervised experiments and analysis. M.O., L.C.S., C.O., S.B.S., and L.F. wrote the manuscript together with all co-authors. All co-authors critically reviewed the manuscript.

Conflict of interest: L.F. has received institutional research grants from governmental and charity funding agencies and several biomedical companies. P.K. has received research support from several drug and device companies active in atrial fibrillation and has received honoraria from several such companies in the past. L.F. and P.K. are listed as inventors on two patents held by University of Birmingham (Atrial Fibrillation Therapy WO 015140571, Markers for Atrial Fibrillation WO 2016012783).

Data availability

The datasets generated during the current study are available from the corresponding author on reasonable request.

References

1. Fabritz L, Crijns H, Guasch E, Goette A, Hausler KG, Kotecha D *et al.* Dynamic risk assessment to improve quality of care in patients with atrial fibrillation: the 7th AFNET/EHRA consensus conference. *Europace* 2021;**23**:329–44.
2. Fabritz L, Guasch E, Antoniades C, Bardinet I, Benninger G, Betts TR *et al.* Expert consensus document: defining the major health modifiers causing atrial fibrillation: a roadmap to underpin personalized prevention and treatment. *Nat Rev Cardiol* 2016;**13**:230–7.
3. Yoneda ZT, Anderson KC, Quintana JA, O'Neill MJ, Sims RA, Glazer AM *et al.* Early-onset atrial fibrillation and the prevalence of rare variants in cardiomyopathy and arrhythmia genes. *JAMA Cardiol* 2021;**6**:1371–9.
4. Darbar D, Kannankeril PJ, Donahue BS, Kucera G, Stubblefield T, Haines JL *et al.* Cardiac sodium channel (SCN5A) variants associated with atrial fibrillation. *Circulation* 2008;**117**:1927–35.
5. Makiyama T, Akao M, Shizuta S, Doi T, Nishiyama K, Oka Y *et al.* A novel SCN5A gain-of-function mutation M1875T associated with familial atrial fibrillation. *J Am Coll Cardiol* 2008;**52**:1326–34.
6. Skryabin BV, Kummerfeld DM, Gubar L, Seeger B, Kaiser H, Stegemann A *et al.* Pervasive head-to-tail insertions of DNA templates mask desired CRISPR-Cas9-mediated genome editing events. *Sci Adv* 2020;**6**:eaax2941.
7. Silbernagel N, Walecki M, Schafer MK, Kessler M, Zobeiri M, Rinne S *et al.* The VAMP-associated protein VAPB is required for cardiac and neuronal pacemaker channel function. *FASEB J* 2018;**32**:6159–73.
8. Blana A, Kaese S, Fortmüller L, Laakmann S, Damke D, van Bragt K *et al.* Knock-in gain-of-function sodium channel mutation prolongs atrial action potentials and alters atrial vulnerability. *Heart Rhythm* 2010;**7**:1862–9.
9. Winters J, von Braunmuhl ME, Zeemering S, Gilbers M, Brink TT, Scaf B *et al.* JavaCyte, a novel open-source tool for automated quantification of key hallmarks of cardiac structural remodeling. *Sci Rep* 2020;**10**:20074.
10. O'BrienS, Holmes AP, Johnson DM, Kabir SN, O'Shea C, O'Reilly M, *et al.* Increased atrial effectiveness of flecainide conferred by altered biophysical properties of sodium channels. *J Mol Cell Cardiol* 2022;**166**:23–35.
11. Lemoine MD, Duverger JE, Naud P, Chartier D, Qi XY, Comtois P *et al.* Arrhythmogenic left atrial cellular electrophysiology in a murine genetic long QT syndrome model. *Cardiovascu Res* 2011;**92**:67–74.
12. Holmes AP, Yu TY, Tull S, Syeda F, Kuhlmann SM, O'Brien SM *et al.* A regional reduction in Ito and IKACh in the murine posterior left atrial myocardium is associated with action potential prolongation and increased ectopic activity. *PLoS One* 2016;**11**:e0154077.
13. O'Shea C, Holmes AP, Yu TY, Winter J, Wells SP, Correia J *et al.* ElectroMap: high-throughput open-source software for analysis and mapping of cardiac electrophysiology. *Sci Rep* 2019;**9**:1389.
14. Ramos E, O'Leary ME. State-dependent trapping of flecainide in the cardiac sodium channel. *J Physiol* 2004;**560**:37–49.
15. Remme CA, Verkerk AO, Nuyens D, van Ginneken AC, van Brunschot S, Belterman CN *et al.* Overlap syndrome of cardiac sodium channel disease in mice carrying the equivalent mutation of human SCN5A-1795insD. *Circulation* 2006;**114**:2584–94.
16. Clerx M, Heijman J, Collins P, Volders PGA. Predicting changes to INa from missense mutations in human SCN5A. *Sci Rep* 2018;**8**:12797.
17. Nathan S, Gabelli SB, Yoder JB, Srinivasan L, Aldrich RW, Tomaselli GF *et al.* Structural basis of cytoplasmic NaV1.5 and NaV1.4 regulation. *J Gen Physiol* 2021;**153**:e202012722.
18. Remme CA, Bezzina CR. Sodium channel (dys)function and cardiac arrhythmias. *Cardiovasc Ther* 2010;**28**:287–94.